MR of diffusion slowing in global cerebral ischemia.

A Bizzi, A Righini, R Turner, D LeBihan, D DesPres, G Di Chiro and J R Alger

AJNR Am J Neuroradiol 1993, 14 (6) 1347-1354
http://www.ajnr.org/content/14/6/1347

MR of Diffusion Slowing in Global Cerebral Ischemia

Alberto Bizzi,[1] Andrea Righini,[1] Robert Turner,[2] Denis LeBihan,[3] Daryl DesPres,[4] Giovanni Di Chiro,[1] and Jeffry R. Alger[1]

PURPOSE: To investigate the causal connections between ischemia and the hyperintensity in diffusion-weighted MR images that has been associated with it. **METHODS:** Diffusion-weighted and T2-weighted MR imaging were used in a feline global cerebral ischemia/reperfusion model. Single 30-minute vascular occlusions followed by reperfusion were studied. Global occlusions were used to avoid interpretive complications associated with the temporally unstable hemodynamics of the penumbral zones around focal occlusions and the possible growth of the ischemic and penumbral regions with time. **RESULTS:** Diffusion-weighted hyperintensity and the associated diffusional slowing were not attributable exclusively to the cessation of blood flow because: 1) it does not appear abruptly at the onset of ischemia; 2) it resolves slowly early in reperfusion; and 3) it reappears after prolonged reperfusion. **CONCLUSION:** The times during which diffusion-weighted hyperintensity is manifested during ischemia, and recovers with reperfusion, point to a role for energy metabolism failure.

Index terms: Brain, ischemia; Brain, magnetic resonance; Magnetic resonance, diffusion-weighted scanning; Magnetic resonance, experimental; Animal studies

AJNR 14:1347–1354, Nov/Dec 1993

Diffusion-weighted spin-echo (DWSE) magnetic resonance (MR) (1, 2) has been shown to be sensitive to ischemic brain injuries in studies in which DWSE MR measurements were performed in cats and rats after focal occlusion of the cerebral vasculature (3–13). These studies have shown that ischemic cerebral tissue produces abnormally hyperintense signal in diffusion-weighted MR imaging earlier in the infarction process than in conventional T2-weighted MR imaging. A recent study of stroke patients has provided a further confirmation (14). The results are consistent with the slowing of the random diffusional motions of the water molecules in the damaged tissue, but the underlying pathophysiologic processes that induce the diffusional slowing have yet to be clearly elucidated (2, 7).

The goal of the present work was to make sequential DWSE MR measurements during ischemia and reperfusion to improve our understanding of the causal connections between cerebral ischemia and the slowed diffusion. Specifically, we sought to establish whether the diffusional slowing occurred abruptly at the onset of ischemia and quickly recovered with reperfusion. A demonstration that the ischemic hyperintensity in the diffusion-weighted images develops instantaneously with ischemia would lead to the conclusion that it is causally associated with ischemia per se, whereas a slower contrast development would implicate a slower process that is only initiated by ischemia.

Received August 28, 1992; revision requested October 22, received and accepted November 16.

[1] Neuroimaging Branch, National Institute of Neurological Disorders and Stroke, [2] Laboratory of Cardiac Energetics, National Heart, Lung, and Blood Institute, [3] Department of Diagnostic Radiology, Warren G. Magnuson Clinical Center, and [4] Biomedical Engineering and Instrumentation Program, National Center for Research Resources, National Institutes of Health, Bethesda, MD 20892.

Address reprint requests to Jeffry R. Alger, PhD, NIH Bldg 10, Room B1D-121, Bethesda, MD 20892.

AJNR 14:1347–1354, Nov/Dec 1993 0195-6108/93/1406–1347

Materials and Methods

Animal Preparation

Animal studies were performed in compliance with National Institutes of Health guidelines after approval by the relevant local committees. Adult cats (3.0–4.0 kg) were tranquilized with ketamine (15 mg/kg administered intramuscularly) and then anesthetized with 2% to 3% halothane in 30% O_2 and 70% N_2O applied via a face mask. After endotracheal intubation and placement of catheters

in a femoral artery and a femoral vein, the animals were immobilized with a constant intravenous infusion of 3 to 6 mg/kg per hour succinylcholine chloride and ventilated mechanically with 1% to 2% halothane in 30% O_2 and 70% N_2O. The tidal volume was adjusted to produce P_aO_2 of 100 torr or greater and P_aCO_2 of 30 to 40 torr. Temperature support was provided by a thermostat-controlled, circulating-water heating pad placed around the body. These conditions were maintained throughout the subsequent surgery for placement of the arterial occluders and the MR studies. Arterial blood pressure was monitored throughout the study. Arterial blood samples were withdrawn for measurement of pH and blood gases periodically.

Ischemia

Global cerebral ischemia was produced by reversible intrathoracic occlusion of the innominate and left subclavian arteries, which supply both carotid and vertebral arteries in the cat. For this purpose, a midsternum thoracotomy was performed, and the vessels exposed at their origin from the aortic arch were surrounded by fluid-filled vascular occluders (In Vivo Metric, Healdsburg, Calif), which could be inflated by remote application of pressure on the catheters connected to the occluders. Before occluder placement, the internal mammary arteries were permanently ligated to prevent collateral blood supply to the subclavian arteries. After placement of the occluders, the sternum was closed with sutures, and the head was placed within the radio-frequency coil with the animal in a supine position to minimize motion artifacts (10). Two reference samples, one containing distilled water and the other containing corn oil, were placed beside the head to provide invariant signal-intensity references. Two groups were examined. The 30-min ischemia group (n = 5) received a 30-min episode of global cerebral ischemia followed by reperfusion. The control group (n = 3) had surgery and occluder placement without ischemia.

MR

MR data were obtained with a General Electric 2.0-T Omega MR system (GE NMR Instruments, Fremont, Calif) with a horizontal clear bore of 35 cm. The system included a self-shielded gradient set capable of producing gradient pulses up to 4.0 gauss/cm. A home-built bird-cage radio-frequency coil (15-cm diameter) was used as transmitter and receiver. The subject was centered in the magnet/gradient system with the aid of T1-weighted MR images and not moved for the remainder of the study. T2-weighted spin-echo (T2WSE) MR imaging was performed in the coronal plane using the standard imaging pulse program provided by the manufacturer (GE NMR Instruments, Fremont, Calif). Typically, acquisitions were obtained using the following parameters: 8 sections, 2800/80/2 (repetition time/echo time/excitations), 2-mm section thickness, 2-mm section gaps, 120-mm field of view, 128 phase-encode steps, and 256 points per echo. Image data were filtered, zero filled to 256^2, Fourier transformed, and magnitude corrected with the Omega MR system. DWSE MR was performed using the same parameters used for the T2WSE MR, with the addition of a pair of strong gradient pulses (30-msec duration) during the echo time intervals. The "y" gradient (ventral-dorsal axis) was used for the diffusion-weighting pulses in all cases. The "b" value (2), in the y direction for the entire sequence, was calculated to be 740 seconds/mm. The b values along other axes were negligible.

Region-of-Interest Analysis

T2WSE MR and DWSE MR images were transferred to a Macintosh computer (Apple Computer, Cupertino, Calif) where region-of-interest (ROI) analysis was performed with the NIH-IMAGE program (National Institutes of Health, Bethesda, MD). Global as well as focal ROI measurements were performed. For the global ROI analysis, the signal intensity from all brain parenchyma in the four sections centered around the thalamic nuclei was measured at each time point, normalized to the oil-reference sample's intensity for that section, and averaged. The volume-averaged signal intensities were then normalized for each subject to those obtained before ischemia. This global ROI analysis was designed to give a picture of the temporal changes in the DWSE MR signal intensity for all cerebral tissue and was appropriate given the global nature of the ischemia. Its primary potential shortcoming is the underestimation of the magnitude of the changes in ischemia-sensitive tissues through averaging with less sensitive tissues. Data from different subjects obtained during specific time windows relative to the occlusion were pooled for statistical analysis. For the focal ROI analysis, relevant anatomic structures (lateral gyrus gray matter and basal ganglia) were identified in single sections of the preischemic T2WSE MR images. The signal mean intensities of these regions were then obtained from the DWSE MR data. Each individual measurement was first normalized to the signal intensity of the oil-reference sample and then normalized to the preischemic measurement.

Apparent Diffusion Coefficients

The theory behind computing Apparent Diffusion Coefficients (ADCs) from diffusion-weighted MR data has been previously described (2). ADC images of selected sections in selected subjects were computed using a two-point method. A DWSE MR data set (b = 740 sec/mm^2) and a single T2WSE MR data set (b = 0 sec/mm^2) from the same section provided the raw data for these computations. The ADC in each volume element in the images was obtained by dividing the difference in the logarithm of the signal intensity between the two images by the difference in the b values (740 sec/mm^2) used to acquire the two images. The ADC images were then formed from the ADC values obtained from each of the volume elements by assigning a gray level (white indicates higher ADC) to the values. A previously described program (15) was used to perform the calculations. The relatively slow spin-echo imaging meth-

ods, and the need to archive data periodically, necessitated a finite time separation between collection of the two component images used for the computation. Alternative more rapid methods based on diffusion-weighted echo-planar MR (2, 16, 17) were not used because they produced anatomic images of lower quality than spin-echo methods, and because a pulse program capable of multiple section data collection was not readily available. In general, ADCs were calculated using component images that were acquired within 15 minutes of each other. The ADC computations made for the preischemic and ischemic periods represented exceptions, as they were made using preischemic T2WSE MR data.

Results

Control Group

Three control subjects were studied with DWSE MR and T2WSE MR for periods up to 24 hours. No remarkable changes in the DWSE MR signal intensities were observed in any of the three subjects. Results of the ROI analyses from these subjects are shown in the figures illustrating the ROI analyses of the ischemia-group images (see below).

Thirty-Minute Ischemia Group

Thirty-minute vascular occlusions followed by reperfusion were performed in five subjects. Four of these studies yielded interpretable DWSE MR data, with motion artifacts precluding the analysis of the data from one subject. Representative data from a section through the thalamic nuclei from one of the subjects showing the diffusion-weighted signal intensity changes from preischemia to reperfusion are displayed in Figure 1. Before occlusion (control image, −7 minutes), the signal characteristics of normal brain (hyperintense gray matter relative to white matter and cerebrospinal fluid) were consistent with previous reports (4, 9, 12, 13, 17, 18). During the occlusion (ischemic, +23 minutes), a slow increase in the signal intensity of cortical gray matter and basal ganglia with no substantial change in the white-matter signal intensity was observed. During the first hour of reperfusion (reflow, +63 minutes), there was a slow, partial return to the preischemic appearance, followed by a bilateral increase in the signal intensity from the gray matter of the lateral gyri and the dorsal hippocampi (reflow, +139 minutes). By 4 hours after occlusion the hyperintensity spread to the suprasylvian gyrus, without any noticeable change in the white-matter tracts (reflow, 265 minutes). At 9 to 10 hours after occlusion (reflow, 577 minutes), there was diffuse gray-matter hyperintensity, and compression of the cerebrospinal fluid spaces was apparent.

The results of the global ROI analysis appear in Figure 2. The two measurements made before ischemia, and those made in the control subjects, reveal that the measurement variance in the normalized signal intensity is small relative to the changes brought about by ischemia. The mean signal intensity measured from the latter of the two acquisitions made during ischemia is significantly higher than that measured from the earlier one ($P < .05$, Student t test, Bonferroni correction). The early ischemic measurements (9–13 minutes) are not significantly different from the preischemic control measurements, whereas the later measurements made during ischemia (21–27 minutes) are significantly higher than preischemic measurements ($P < .05$, Student t test, Bonferroni correction). Notice that reperfusion does not bring about an abrupt return of the signal intensity to preischemic values. Measurements made during the first hour of reperfusion show that the signal intensity remains significantly elevated relative to control ($P < .05$, Student t test, Bonferroni correction). The average signal increase during ischemia is on the order of 20%, and the immediate reperfusion interval is characterized by an average signal increase relative to the preischemic values of 10% to 20%. These results reveal that the DWSE MR signal intensity does not abruptly increase with the onset of ischemia, nor does it return to normal immediately with reperfusion.

The results of the focal ROI analysis appear in Figure 3. The evolution of the normalized DWSE MR signal intensity in the basal ganglia (Fig 3A) and gray matter of the lateral gyrus (Fig 3B) are shown for each of the four subjects. The scatter in these data is larger than that shown in Figure 2 because the ROIs are smaller in area and are, thus, more markedly influenced by noise and motion artifacts. Although analysis of these data do not allow statistically relevant conclusions, they qualitatively support the conclusions made from the global ROI analysis. In each case, the signal intensity determined from the latter of the two images obtained during ischemia is larger than that obtained from the first ischemic image. Moreover, none of these measurements provides any evidence of an abrupt return of the signal intensity to normal with reperfusion.

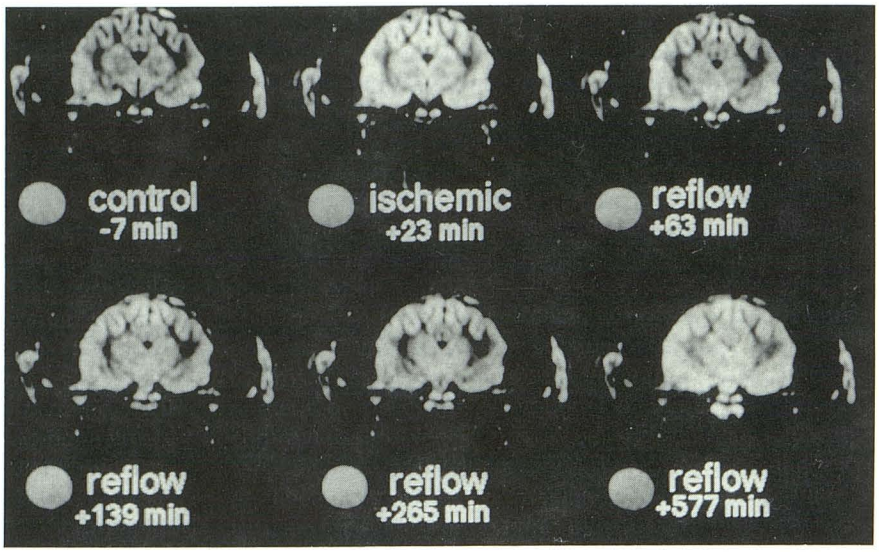

Fig. 1. Representative DWSE MR data from one subject in the 30-min ischemia group. Selected images (acquisition conditions given in Materials and Methods) taken at the times indicated (beginning of occlusion to the midpoint of image acquisition) from 2-mm-thick sections are shown. The standard containing corn oil is evident *below* and to the *left* of each image. The temporal invariance in the intensity of the sample and the surface fat rule out complicating time-dependent intensity variations arising from instrumental causes. The higher intensity of the more viscous corn oil sample (slower diffusion than water) verifies that the images are diffusion weighted.

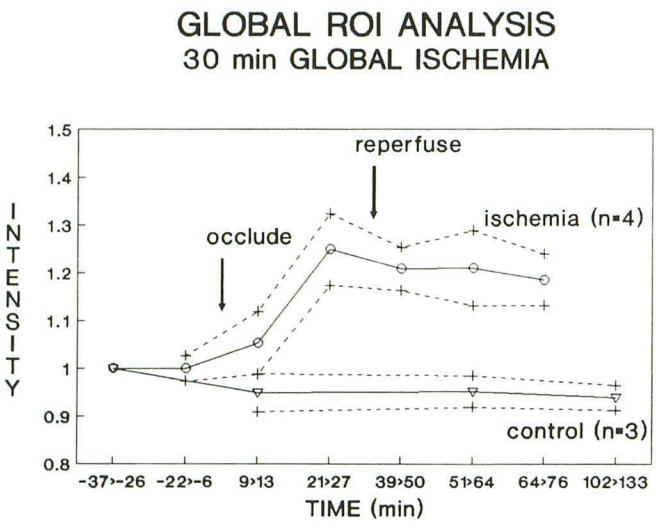

Fig. 2. Temporal behavior of the normalized total-brain DWSE MR signal intensity during ischemia and early reperfusion in the 30-min ischemia group (n = 4) and the control group (n = 3). See Materials and Methods for ROI analysis procedures. Means are shown as *circles connected by solid lines. Dashed lines* and + *symbols* denote 1 SD from the means.

The signal intensities in the DWSE MR images shown in Figure 1 and used for the ROI analyses are dependent on T2 and the ADC. The effects of these two parameters may be separated if T2WSE MR data are available (see Materials and Methods). T2WSE MR measurements were not made with the same frequency as the DWSE MR measurements, because our primary goal was to describe the evolution of the DWSE MR data. Also, previous studies have shown T2WSE MR to be relatively insensitive to acute ischemia (6, 10, 13, 19–21), and our T2WSE MR data (data not shown) are consistent with these previous reports, in that no substantial variations were observed until hours after the occlusion/reperfusion procedures. In all cases the earliest postischemic T2WSE MR was indistinguishable from that obtained before ischemia. The ADC images shown in Figure 4 were computed for the subject whose images appear in Figure 1, using DWSE MR and T2WSE MR data (see Materials and Methods). These calculated images demonstrate a uniform decrease in the ADC in cortex, hippocampus, and basal ganglia during ischemia (ischemic, +24 min). However, the white-matter ADC obtained during ischemia is similar to that measured in the preischemic period. The first hour of reperfusion is characterized by a slow trend toward recovery, but the image obtained at 97 minutes shows that the ADC in the parts of the basal ganglia has not yet returned to its preischemic value. Subsequently, a bilateral decreased ADC in the lateral gyri becomes apparent (reflow, +279 min). This is followed by a diffuse decrease in the ADC (reflow, +577 min). The mean numerical ADC values with standard deviations of selected tissues at selected times are provided in Table 1. These data show that the ADCs of ischemia-sensitive tissue are decreased by 10% to 30% by the end of the ischemic period (21.7 minutes) and then drop further after prolonged reperfusion, reaching close to 50% of the control value in some tissues (particularly the lateral gyri) by the conclusion of the study.

Discussion

In contrast to earlier studies (3–13), a focal brain ischemia model was not used in our study.

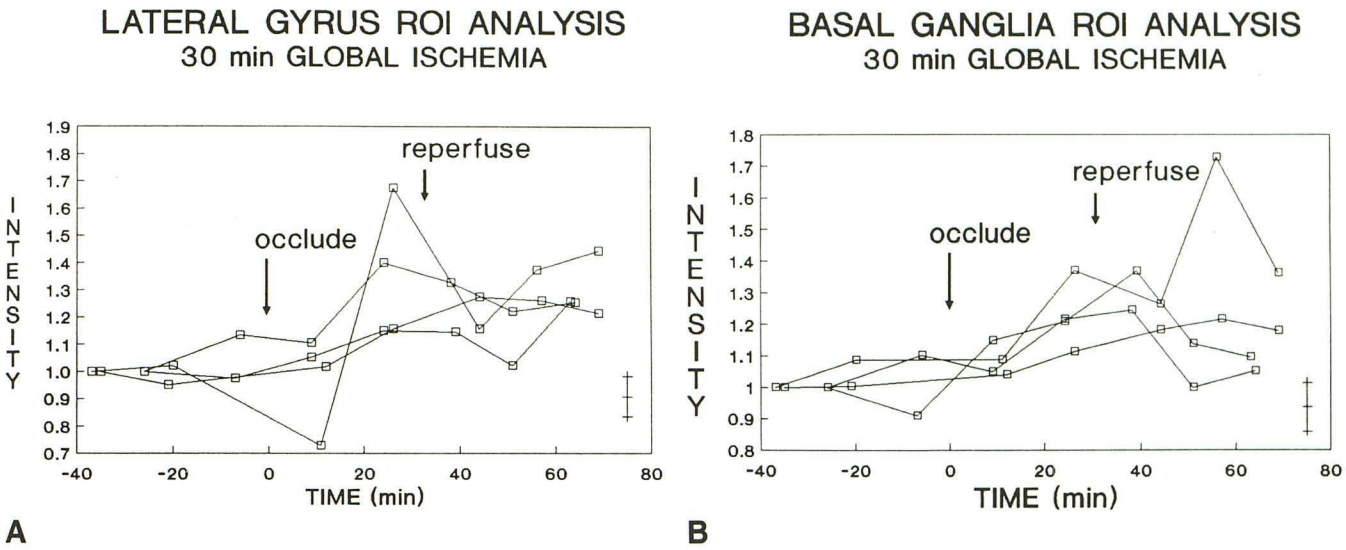

Fig. 3. Temporal behavior of the normalized signal intensity from ROIs placed in the lateral gyrus (*A*) and basal ganglia (*B*). See Materials and Methods for ROI analysis procedures. The results from the four separate subjects are shown as *squares connected by solid lines*. Movement artifacts in the images obtained during the occlusion were responsible for the large deviations shown for one subject. The mean ± 1 SD for the same ROIs in the control group are shown in the *lower right* corner of each plot.

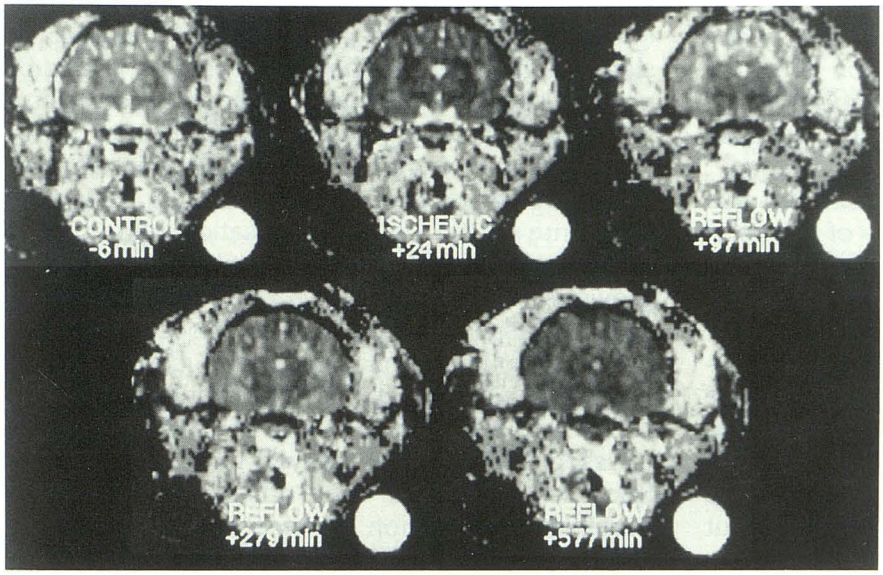

Fig. 4. Representative calculated images of the ADC taken from the same study and image plane shown in Figure 1 (See Materials and Methods for details). Larger ADC's are shown as more intense signals. The times at which the DWSE MR component images were obtained (beginning of occlusion to the midpoint of image acquisition) are shown *below* each image. The standard containing water is evident *below* and to the *right* of each image. The time between the acquisition of the T2WSE MR component image and the DWSE MR component image was less than 15 min for the three reflow images. The T2WSE MR component image used for the calculation of the control and ischemic images was obtained 160 min before the occlusion.

TABLE 1: Mean ADCs, 30-min vascular occlusion

Time[a]	n	Lateral Gyrus[b]	Hippocampus[b]	White Matter[b]	Thalamus[b]
−20.5 (11.8)	4	1.11 (0.11)	1.08 (0.22)	1.03 (0.09)	0.89 (0.12)
21.7 (2.2)	4	0.94 (0.26)	0.92 (0.38)	0.75 (0.10)	0.76 (0.26)
80.7 (12.0)	4	0.58 (0.16)[c]	0.75 (0.21)	0.99 (0.34)	0.68 (0.22)
157.0 (19.1)	3	0.67 (0.19)	0.69 (0.14)	0.73 (0.30)	0.68 (0.36)
272.3 (6.5)	3	0.56 (0.14)[c]	0.75 (0.16)	0.87 (0.29)	0.74 (0.34)

[a] Values in minutes with standard deviations given in parentheses.

[b] Values in millimeters squared per second × 10^{-3} with standard deviations given in parentheses.

[c] Significant relative to control period ($P < .05$, Student t test, Bonferroni correction).

Instead, we used a reversible extracranial vascular occlusion model (22–28) that produces global cerebral ischemia. This model allows one to manipulate blood flow after the subject has been positioned in the magnet and thereby permits image acquisition in the very early stages of ischemia and reperfusion. A second rationale for using a global cerebral ischemia model is that one is not presented with the problems related to the interpretation of changes in diffusion properties connected with the complex and temporally unstable hemodynamics in the vicinity of a focal occlusion (29–34). Soon after the onset of focal ischemia a luxury hyperperfusion may be expected in the ischemic penumbra, with possible later development of hypoperfusion. Juxtaposed to this is the ischemic core where blood flow is, by definition, zero. Given the limited spatial resolution of MR (particularly in the direction perpendicular to the imaging plane), it would be problematic to differentiate temporal changes in the DWSE MR signal intensity arising from the evolution of the hemodynamic conditions in these two tissue volumes from changes caused by the growth in their volumes. Interpretation of signal intensity changes with a controlled global ischemia model is far more straightforward, because partial volume effects exert a smaller influence.

The vascular occlusion model used in this study permits the global inhibition of cerebral blood flow to values well below the ischemic threshold for functional failure in a matter of seconds (22, 23, 25, 28). Furthermore, the ability to reperfuse in a few seconds, even after prolonged ischemia, to a normo- to hyperemic state by releasing the occlusion is well documented (25, 26). A hypoperfused state, which may persist for many hours, characterized by a cerebral blood flow of about 50% of control values and without CO_2 reactivity, eventually develops with reperfusion (24, 26). During the hypoperfusion, the cerebral blood flow is sufficient for the recovery of aerobic energy metabolism (27, 28), but the lack of CO_2 reactivity may put the tissue at risk of secondary metabolic failure because the blood flow is low and may not be sufficient to compensate for renewed oxygen and glucose demands as the tissue begins to function.

In this study, DWSE MR measurements were made during the ischemic and postischemic states. The model used here permits one to determine whether diffusional slowing occurs abruptly with ischemia and abruptly recovers with reperfusion. The three primary findings are: 1) the ischemia-associated hyperintensity in DWSE MR measurements does not appear instantaneously at the onset of cerebral ischemia; 2) the hyperintensity does not resolve instantaneously with reperfusion after prolonged ischemia; and 3) the hyperintensity may reappear later during reperfusion. Thus, we have confirmed with a global ischemia model previous findings with focal models (3–13) that abnormal diffusion properties are associated with ischemia. Furthermore, we have shown that the temporal correlation between the development and/or resolution of abnormal diffusion properties and the initiation of ischemia or reperfusion is not close. These findings are consistent with recent studies that show a noninstantaneous diffusional slowing with the onset of focal ischemia (4). Our observations lead to the conclusion that the causal associations between the abnormal diffusion properties and ischemia are indirect. The diffusional slowing must be brought about by some ischemia-elicited pathophysiologic mechanism or mechanisms, which: 1) take place several minutes after the onset of ischemia to be manifested; 2) resolve slowly during the first hour of reperfusion; and 3) may redevelop at later times during reperfusion.

The observation that ischemia-elicited diffusion-weighted hyperintensity is not directly associated with ischemia per se permits us to rule out some of the possible causation hypotheses, such as decreased tissue pulsatility discussed in previous publications (2, 7, 10). One hypothesis that is consistent with the present observations is the "cytotoxic edema hypothesis" (35), in which the cellular swelling that results from energy failure followed by the failure of ion homeostasis is associated with the slowed random diffusion. Such an association may arise in a number of possible ways. As ion homeostasis fails, water is redistributed from the extracellular compartment, where diffusion may be less restricted, to the intracellular space, where it may be more restricted because of the presence of limiting membranes and to a generally more viscous environment. Alternatively, as ion homeostasis fails and the cells swell, there may be a decrease in the membrane water permeability because of membrane structural changes. In either case, the consistency of the present observations with the cytotoxic edema hypothesis arises from the fact that ion homeostasis does not fail immediately at the onset of ischemia but occurs more slowly, as the energy-yielding adenosine triphosphate pool is depleted (36–39). The adenosine triphosphate

pool is depleted during the first few minutes of ischemia (27, 28, 37, 40–46) and shows a slow recovery during reperfusion after prolonged ischemia (27, 28, 37, 40, 44, 46). These time features generally fit with the temporal behavior of the DWSE MR properties observed here. The hypothesis is also supported by studies in which the cytotoxic edema associated with focal ischemia was modulated pharmacologically (7), by studies in which a sodium-calcium ion channel modulator reduced the size of the hyperintense volumes seen on diffusion-weighted MR images after focal cerebral occlusions (9), and by studies in which kainic acid injection, without ischemia, led to hyperintensity in diffusion-weighted MR images (47). It also has been supported by correlated measurements of diffusion-weighted hyperintensity and adenosine triphosphatase activity, in a focal ischemia model (48).

Our results demonstrate that diffusion-weighted MR hyperintensity can redevelop during the reperfusion period after global cerebral ischemia. Furthermore, we have found (Fig 4 and Table 1) that the ADCs are decreased to a greater extent during the late-reperfusion period than they are during the occlusion. The discussion above would suggest that the development of diffusion-weighted hyperintensity during the reperfusion should correlate with a failure in energy metabolism. Previous studies using this model (27) have shown evidence for energy metabolism failure after successful reperfusion and repletion of the ATP pool. This reasoning underscores the need for combined MR spectroscopic and DWSE MR observations during the reperfusion period.

Acknowledgments

This work was performed in the National Institutes of Health In Vivo NMR Research Center. Dr Carlo Pierpaoli, Dr James Matiello, and Ms Carol Haslem provided technical assistance.

References

1. Le Bihan D, Breton E, Lallamand D, Grenier P, Cabanis E, Laval-Jeantet M. MR imaging of intravoxel incoherent motions: application to diffusion and perfusion in neurologic disorders. *Radiology* 1986;161:401–407
2. Le Bihan D. Molecular diffusion nuclear magnetic resonance imaging. *Magn Reson Q* 1991;7:1–30
3. Moseley ME, Kucharczyk J, Mintorovitch J, et al. Diffusion-weighted MR imaging of acute stroke: correlation with T2-weighted and magnetic susceptibility-enhanced MR imaging in cats. *AJNR: Am J Neuroradiol* 1990;11:423–429
4. Kucharczyk J, Mintorovitch J, Asgari HS, Moseley M. Diffusion/perfusion MR imaging of acute cerebral ischemia. *Magn Reson Med* 1991;19:311–315
5. Knight RA, Ordidge RJ, Helpern JA, Chopp M, Rodolosi LC, Peck D. Temporal evolution of ischemic damage in rat brain measured by proton nuclear magnetic resonance imaging. *Stroke* 1991;22:802–808
6. van Bruggen N, Cullen BM, King MD, et al. T2- and diffusion-weighted magnetic resonance imaging of a focal ischemic lesion in rat brain. *Stroke* 1992;23:576–582
7. Benveniste H, Hedlund LW, Johnson GA. Mechanism of detection of acute cerebral ischemia in rats by diffusion-weighted magnetic resonance microscopy. *Stroke* 1992;23:746–754
8. Berry I, Gigaud M, Manelfe C. Experimental focal cerebral ischaemia assessed with IVIM-MRI in the acute phase at 0.5 tesla. *Neuroradiology* 1992;34:134–139
9. Kucharczyk J, Mintorovitch J, Moseley ME, et al. Ischemic brain damage: reduction by sodium-calcium ion channel modulator RS-87476. *Radiology* 1991;179:221–227
10. Mintorovitch J, Moseley ME, Chileuitt L, Shimizu H, Cohen Y, Weinstein PR. Comparison of diffusion- and T2-weighted MRI for the early detection of cerebral ischemia and reperfusion in rats. *Magn Reson Med* 1991;18:39–50
11. Minematsu K, Li L, Fisher M, Sotak CH, Davis MA, Fiandaca MS. Diffusion-weighted magnetic resonance imaging: rapid and quantitative detection of focal brain ischemia. *Neurology* 1992;42:235–240
12. Moseley ME, Cohen Y, Mintorovitch J, et al. Early detection of regional cerebral ischemic injury in cats: evaluation of diffusion and T2-weighted MRI and spectroscopy. *Magn Reson Med* 1990;14:330–346
13. Moonen CTW, Pekar J, De Vleeschouwer MHM, Van Gelderen P, van Zijl PCM, DesPres D. Restricted and anisotropic displacement of water in healthy cat brain and in stroke studied by NMR diffusion imaging. *Magn Reson Med* 1991;19:327–332
14. Chien D, Kwong KK, Gress DR, Buonanno FS, Buxton RB, Rosen BR. MR diffusion imaging of cerebral infarction in humans. *AJNR: Am J Neuroradiol* 1992;13:1097–1102
15. Goldberg R, Le Bihan D. Interactive data processing for magnetic resonance imaging: application to diffusion and perfusion imaging. In: Brody WR, Johnston GS, eds. *Computer applications to assist radiology* Carlsbad, Calif: Symposia Foundation, 1992:384
16. Wendland MF, White DL, Aicher KP, Tzika AA, Moseley ME. Detection with echo-planar MR imaging of transit of susceptibility contrast medium in a rat model of regional brain ischemia. *Magn Reson Imaging* 1991;1:285–292
17. Le Bihan D, Turner R, Moonen CTW, Pekar J. Imaging of diffusion and microcirculation with gradient sensitization: design, strategy and significance. *Magn Reson Imaging* 1991;1:7–28
18. Le Bihan D, Moonen CTW, van Zijl PCM, Pekar J, DesPres D. Measuring random microscopic motion of water in tissues with MR imaging: a cat brain study. *J Comput Assist Tomogr* 1991;15:19–25
19. Brant-Zawadzki M, Pereira B, Weinstein P, et al. MR imaging of acute experimental ischemia in cats. *AJNR: Am J Neuroradiol* 1986;7:7–11
20. Bose B, Jones SC, Lorig R, Friel HT, Weinstein M, Little JR. Evolving focal cerebral ischemia in cats: spatial correlation of nuclear magnetic resonance imaging, cerebral blood flow, tetrazolium staining, and histopathology. *Stroke* 1988;19:28–37
21. Alberts MJ, Faulstisch ME, Gray L. Stroke with negative brain magnetic resonance imaging. *Stroke* 1992;23:663–667
22. Hossmann KA, Kleihues P. Reversibility of ischemic brain damage. *Arch Neurol* 1973;29:375–384
23. Schmidt-Kastner R, Hossmann K-A, Grosse-Ophoff B. Relationship between metabolic recovery and the EEG after prolonged ischemia of cat brain. *Stroke* 1986;17:1164–1169

24. Schmidt-Kastner R, Hossmann K-A, Grosse Ophoff B. Pial artery pressure after one hour of global ischemia. *J Cereb Blood Flow Metab* 1987;7:109–117
25. Hossmann K-A, Lechtape-Grueter H, Hossmann V. The role of cerebral blood flow for the recovery of the brain after prolonged ischemia. *Z Neurol* 1973;204:281–299
26. Brunetti A, Nagashima G, Bizzi A, DesPres D, Alger JR. Cerebral blood flow in experimental ischemia assessed by ^{19}F magnetic resonance spectroscopy in cats. *Stroke* 1990;21:1439–1444
27. Behar KL, Rothman DL, Hossmann K-A. NMR spectroscopic investigation of the recovery of energy and acid-base homeostasis in the cat brain after prolonged ischemia. *J Cereb Blood Flow Metab* 1989;9:655–665
28. Alger JR, Brunetti A, Nagashima G, Hossmann K-A. Assessment of post-ischemic cerebral energy metabolism in cat by P-31 NMR: the cumulative effects of secondary hypoxia and ischemia. *J Cereb Blood Flow Metab* 1989;9:506–514
29. Baron JC, Frackowiak RSJ, Herholz K, et al. Use of PET methods for measurement of cerebral energy metabolism and hemodynamic in cerebrovascular disease. *J Cereb Blood Flow Metab* 1989;9:723–742
30. Hossmann K-A, Mies G, Paschen W, et al. Multiparametric imaging of blood flow and metabolism after middle cerebral artery occlusion in cats. *J Cereb Blood Flow Metab* 1985;5:97–107
31. Pulsinelli WA, Levy DE, Duffy TE. Regional cerebral blood flow and glucose metabolism following transient forebrain ischemia. *Ann Neurol* 1982;11:499–509
32. Kagstrom E, Smith M-L, Siesjö BK. Local cerebral blood flow in the recovery period following complete cerebral ischemia in the rat. *J Cereb Blood Flow Metab* 1983;3:170–182
33. Kuhl DE, Phelps ME, Kowell AP, Metter EJ, Selin C, Winter J. Effects of stroke on local cerebral metabolism and perfusion: mapping by emission computed tomography of ^{18}FDG and $^{13}NH_3$. *Ann Neurol* 1980;8:47–60
34. Heiss W-D, Huber M, Fink GR, et al. Progressive derangement of periinfarct viable tissue in ischemic stroke. *J Cereb Blood Flow Metab* 1992;12:193–203
35. Klatzo I. Neuropathological aspects of brain edema. *J Neuropathol Exp Neurol* 1967;26:1–13
36. Gyulai L, Schnall M, McLaughlin AC, Leigh JS Jr, Chance B. Simultaneous ^{31}P- and ^{1}H-nuclear magnetic resonance studies of hypoxia and ischemia in the cat brain. *J Cereb Blood Flow Metab* 1987;7:543–551
37. Eleff SM, Maruki Y, Monsein LH, Traystman RJ, Bryan RN, Koehler RC. Sodium, ATP, and intracellular pH transients during reversible complete ischemia of dog cerebrum. *Stroke* 1991;22:233–241
38. Naritomi H, Sasaki M, Kanashiro M, Kitani M, Sawada T. Flow thresholds for cerebral energy disturbance and Na^+ pump failure as studied by in vivo ^{31P} and ^{23}Na nuclear magnetic resonance spectroscopy. *J Cereb Blood Flow Metab* 1988;8:16–23
39. Hansen AJ. Effect of anoxia on ion distribution in the brain. *Physiol Rev* 1985;65:101–148
40. Widmer H, Abiko H, Faden AI, James TL, Weinstein PR. Effects of hyperglycemia on the time course of changes in energy metabolism and pH during global cerebral ischemia and reperfusion in rats: correlation of ^{1}H and ^{31}P NMR spectroscopy with fatty acid and excitatory amino acid levels. *J Cereb Blood Flow Metab* 1992;12:456–468
41. Hilberman M, Hariharasubramanian V, Haselgrove J, Cone JB, Gyulai L, Chance B. In vivo time-resolved brain phosphorous nuclear magnetic resonance. *J Cereb Blood Flow Metab* 1984;4:334–342
42. Gadian DG, Frackowiak RSJ, Crockard HA, et al. Acute cerebral ischemia: concurrent changes in cerebral blood flow, energy metabolism, pH and lactate measured with H2 clearance and P-31 and H-1 nuclear magnetic resonance spectroscopy. I. Methodology. *J Cereb Blood Flow Metab* 1987;7:199–206
43. Horikawa Y, Naruse S, Hirakawa K, Tanaka C, Nishikawa H, Watari H. In vivo studies of energy metabolism in experimental cerebral ischemia using topical magnetic resonance. *J Cereb Blood Flow Metab* 1985;5:235–240
44. Andrews BT, Weinstein PR, Keniry M, Pereira B. Sequential in vivo measurement of cerebral intracellular metabolism with P-31 MRS during global cerebral ischemia and reperfusion in rats. *Neurosurgery* 1987;21:699–708
45. Eklöf B, Siesjö B. The effect of bilateral carotid artery ligation upon the blood flow and the energy state of the rat brain. *Acta Physiol Scand* 1972;86:155–165
46. Nishijima MK, Koehler RC, Hurn PD, et al. Postischemic recovery rate of cerebral ATP, phosphocreatine, pH and evoked potentials. *Am J Physiol* 1989;257:H1860–H1870.
47. King MD, van Bruggen N, Ahier RG, et al. Diffusion-weighted imaging of kianic acid lesions in the rat brain. *Magn Reson Med* 1991;20:158–168
48. Mintorovitch J, Baker LL, Yang GY, et al. Diffusion-weighted hyperintensity in early cerebral ischemia: correlation with brain water and ATPase activity (abstr). In: *Book of abstracts: Society of Magnetic Resonance in Medicine 1991*. Berkeley, Calif: Society of Magnetic Resonance in Medicine, 1991;10:329